

**The electromagnetic dipole operator effect on  $\bar{B} \rightarrow X_s \gamma$  at  $\mathcal{O}(\alpha_s^2)$** I. Blokland<sup>1,2</sup>, A. Czarnecki<sup>1</sup>, M. Misiak<sup>3</sup>, M. Ślusarczyk<sup>1,4</sup>, and F. Tkachov<sup>5</sup>*1) Department of Physics, University of Alberta,  
Edmonton, AB T6G 2J1, Canada**2) Department of Physics and Astronomy,  
University of Victoria, Victoria, BC V8P 5C2, Canada**3) Institute of Theoretical Physics,  
Warsaw University, 00-681 Warszawa, Poland**4) Institute of Physics, Jagiellonian University,  
30-059 Kraków, Poland**5) Institute for Nuclear Research,  
Russian Academy of Sciences,  
Moscow, 117312, Russian Federation*

The flavor-changing electromagnetic dipole operator  $O_7$  gives the dominant contribution to the  $\bar{B} \rightarrow X_s \gamma$  decay rate. We calculate two-loop QCD corrections to its matrix element together with the corresponding bremsstrahlung contributions. The optical theorem is applied, and the relevant imaginary parts of three-loop diagrams are computed following the lines of our recent  $t \rightarrow X_b W$  calculation. The complete result allows us to test the validity of the naive non-abelianization (NNA) approximation that has been previously applied to estimate the NNLO QCD correction to  $\Gamma(\bar{B} \rightarrow X_s \gamma)/\Gamma(\bar{B} \rightarrow X_u e \bar{\nu})$ . When both decay widths are normalized to  $m_{b,R}^5$  in the same renormalization scheme  $R$ , the calculated  $\mathcal{O}(\alpha_s^2)$  correction is sizeable ( $\sim 6\%$ ), and the NNA estimate is about 1/3 too large. On the other hand, when the ratio of the decay widths is written as  $S \times m_{b,\overline{\text{MS}}}^2(m_b)/m_{b,\text{pole}}^2$ , the calculated  $\mathcal{O}(\alpha_s^2)$  correction to  $S$  is at the level of 1% for both the complete and the NNA results.

PACS numbers: 13.40.Hq, 14.65.Fy, 12.38.Bx

**I. INTRODUCTION**

The radiative decay  $b \rightarrow s \gamma$  occurs only through quantum loop effects, similarly to the muon anomalous magnetic moment ( $g_\mu - 2$ ) or radiative hyperon decays [1]. The largest contribution by far to ( $g_\mu - 2$ ) is due to electromagnetic interactions. In contrast, the flavor-changing hyperon ( $s \rightarrow d$ ) and  $\bar{B}$  meson ( $b \rightarrow s$ ) decay amplitudes involve heavy particles such as the  $W$  boson and are consequently very rare. In particular, the  $b \rightarrow s \gamma$  transition can be predicted in the Standard Model with good accuracy, and it offers a relatively low-background probe of possible new phenomena such as supersymmetry (e.g., see Ref. [2]).

High-accuracy measurements of the  $\bar{B} \rightarrow X_s \gamma$  rate in  $B$ -factories [3] warrant sophisticated calculations of high-order Standard Model contributions. Electroweak loop effects, without which this decay would not occur, have now been studied to two-loop accuracy [4, 5, 6, 7, 8]. For the precise determination of the rate, the QCD effects are crucial and are fully known to the next-to-leading order (e.g., see Refs. [9, 10]). Potentially important effects resulting from the binding of the  $b$  quark in the  $\bar{B}$  meson were explored in Ref. [11].

At present, several groups are working at the determination of the next-to-next-to-leading order (NNLO) QCD corrections. A discussion of the various required studies can be found in Ref. [12]. Since that review was published, new ingredients have been provided: all the relevant three-loop anomalous dimensions [13, 14], three-loop matching conditions [15], as well as certain counterterm contributions to the three-loop matrix elements of four-quark operators [16].

Among the most challenging missing quantities are the two- and three-loop matrix elements of several operators. So far, the only complete two-loop  $\mathcal{O}(\alpha_s)$  results exist for the four-quark operators, where one of the loops is a fermion loop [17, 18]. In addition, parts of two- and three-loop  $\mathcal{O}(\alpha_s^2)$  matrix elements, involving gluon vacuum polarization, were found in Ref. [19]. This last result is very important since it automatically determines corrections to the matrix elements of order  $\alpha_s^2 \beta_0$ , where  $\beta_0 = 11 - 2N_f/3$  is a large parameter ( $N_f = 5$  denotes the number of quark species).

In the present paper, we provide the first calculation of full two-loop corrections to the matrix element of the electromagnetic dipole operator  $O_7$  that is responsible for the lowest-order  $b \rightarrow s \gamma$  decay rate. We reproduce the

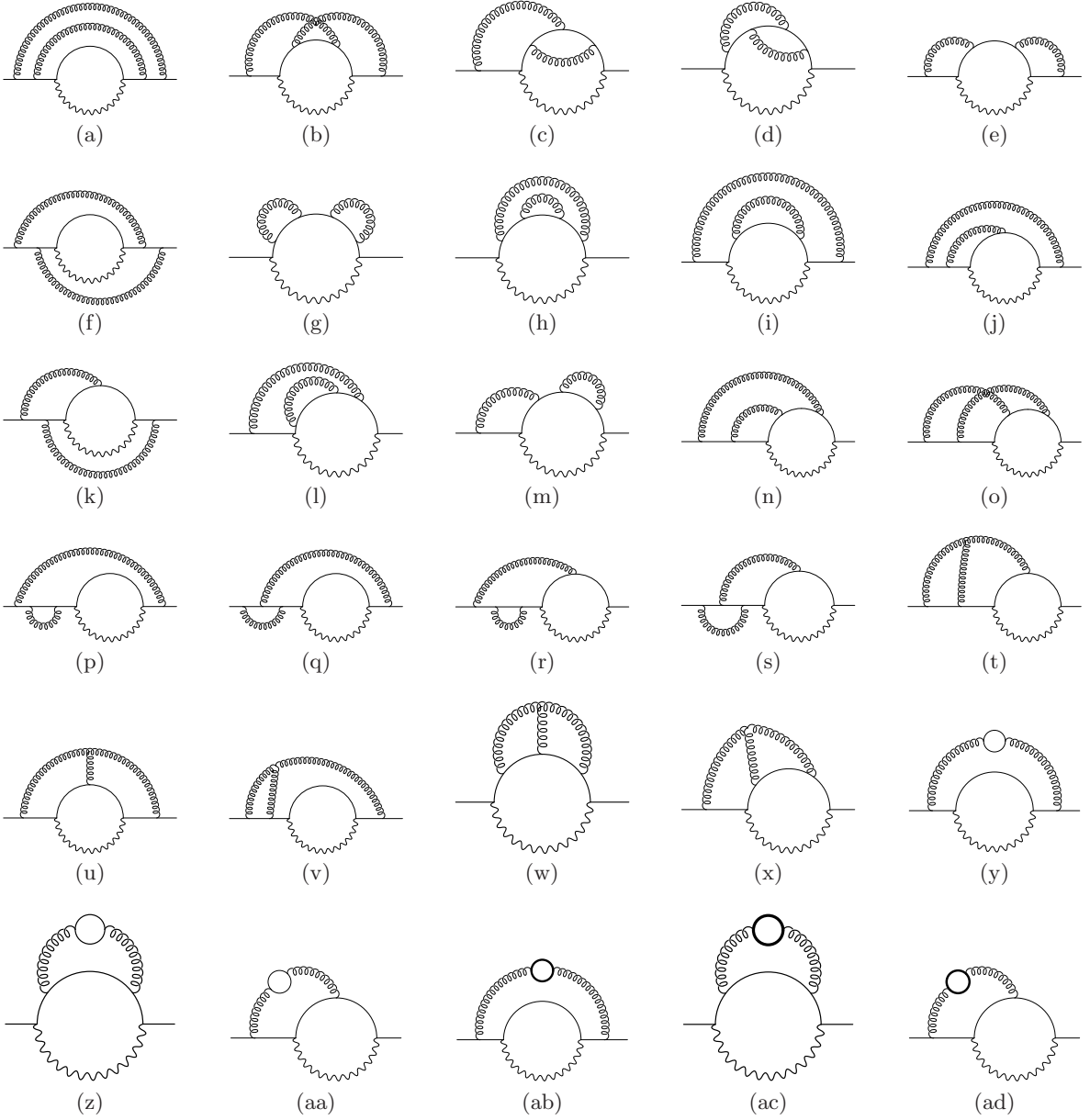


FIG. 1: Three loop self-energy diagrams required for the  $\mathcal{O}(\alpha_s^2)$  computation. Thick solid closed loops in (ab,ac,ad) depict massive ( $b$  quark) loops. Thin solid closed loops in (y), (z), (aa) denote massless fermions. From the latter diagrams we find also the contributions of gluon and ghost loops, as explained in the text.

$\alpha_s^2\beta_0$  effect found in Ref. [19] and also provide the  $\alpha_s^2$  corrections that are not enhanced by  $\beta_0$ . With this result, we can check the extent to which the  $\beta_0$  effect is dominant. The conclusion turns out to depend very much on what renormalization scheme is used for the overall factor of  $m_b^5$  in the expression for the decay rate.

Since the result obtained here is only a partial contribution to the future full NNLO correction, we present a number of intermediate results and describe in detail our renormalization procedure. We hope that this will simplify the utilization of our result when the remaining ingredients are known at the NNLO level.

The paper is organized as follows. In Section II, we describe the calculation of the relevant diagrams as well as their renormalization. Section III is devoted to presenting our main results and discussing the large- $\beta_0$  approximation. We conclude in Section IV. Contributions from particular diagrams are listed in the Appendix.

## II. THE CALCULATION

The decay rate of  $b$  into  $s$ ,  $\gamma$ , and up to two gluons or a light quark pair can be written as

$$\Gamma(b \rightarrow X_s^{\text{parton}} \gamma)_{E_\gamma > E_0} = \frac{G_F^2 \alpha_{\text{em}} m_b^2(\mu) m_b^3}{32\pi^4} |V_{tb} V_{ts}^*|^2 \sum_{i,j} C_i^{\text{eff}}(\mu) C_j^{\text{eff}}(\mu) G_{ij}(E_0, \mu), \quad (1)$$

where  $m_b$  is the pole-mass and  $m_b(\mu)$  is the  $\overline{\text{MS}}$  running mass of the  $b$  quark. The effective [20] Wilson coefficients in the relevant low-energy theory are denoted by  $C_i^{\text{eff}}(\mu)$ . The photon energy cutoff  $E_0$  is assumed to be significantly below the endpoint, i.e.  $m_b - 2E_0 \gg \Lambda_{\text{QCD}}$ . This is a necessary condition for the perturbative decay width (1) to be a good approximation for  $\Gamma(\bar{B} \rightarrow X_s \gamma)_{E_\gamma > E_0}$ .

In this paper, we focus on the contribution of the operator

$$O_7 = \frac{em_b(\mu)}{16\pi^2} \bar{s}_L \sigma^{\mu\nu} b_R F_{\mu\nu} \quad (2)$$

to the decay rate. More specifically, we calculate

$$G_{77}(0, \mu) = 1 + \left( \frac{\alpha_s(\mu)}{4\pi} \right) X_1 + \left( \frac{\alpha_s}{4\pi} \right)^2 X_2 + \mathcal{O}(\alpha_s^3). \quad (3)$$

Our result for  $G_{77}(0, \mu)$  can be combined with the very recent findings of Ref. [21] to obtain  $G_{77}(E_0, \mu)$  at the NNLO for any value of  $E_0$  that is sufficiently far from the endpoint.

As far as the coefficient  $X_1$  is concerned, we confirm the well-known result of Ref. [22]. The NNLO correction  $X_2$  can be subdivided into color structures,

$$X_2 = C_F (T_R N_L X_L + T_R N_H X_H + C_F X_A + C_A X_{NA}) , \quad (4)$$

where  $C_F = 4/3$ ,  $C_A = 3$ , and  $T_R = 1/2$  are the SU(3) color factors, while  $N_L$  and  $N_H$  denote the number of light ( $m_q = 0$ ) and heavy ( $m_q = m_b$ ) quark species ( $N_H + N_L = N_f$ ).

Let us now briefly outline the method applied to the calculation of  $X_2$ . We use the optical theorem to map all the virtual corrections and real radiation contributions onto a system of self-energy diagrams as described in Ref. [23] in the context of the decays  $t \rightarrow X_b W$  and  $b \rightarrow X_u l \bar{\nu}$ . The topologies which have to be taken into account turn out to be identical to those considered there for the top quark decay.

We consider only gluons of virtualities of order  $m_b$ . In the effective theory, this is the only mass scale. In other words, we do not consider hard gluons that would resolve the structure of the effective vertex  $\bar{s} b \gamma$  since their effects are accounted for in the Wilson coefficients  $C_i^{\text{eff}}(\mu)$ . Diagrams needed for the present calculation are analogous to those of the hard asymptotic region for the top quark decay, studied recently in Ref. [23, 24].

Diagrams contributing to  $X_2$  are presented in Fig. 1. All the particles except for the  $b$  quarks are treated as massless. Both the UV and the IR divergences are regulated dimensionally in  $D = 4 - 2\epsilon$  dimensions. The results for  $\mu = m_b$  are collected in Table I in the Appendix along with the relevant color factors. They have been computed in a general covariant gauge. The Feynman gauge results can be obtained by setting  $\xi = 0$ . Diagrams that are not symmetric under left-right reflection are already multiplied by 2. The quantities  $\ln 4\pi$  and  $\gamma$  that account for the difference between the  $\overline{\text{MS}}$  and  $\text{MS}$  schemes are omitted in Table I and in the remainder of this section.

Diagrams with closed gluon or ghost loops are not shown explicitly in Fig. 1, since their contribution can be found from the total contribution of the light fermions. To this end, after computing the light-fermion diagrams, we replace (see for example Ref. [25])

$$T_R N_L \rightarrow T_R N_L - C_A \left[ \frac{5}{4} - \frac{3}{8}\xi + \epsilon \left( \frac{1}{2} + \frac{11}{8}\xi + \frac{3}{16}\xi^2 \right) + \epsilon^2 \left( \frac{1}{2} + \frac{3}{8}\xi + \frac{1}{16}\xi^2 \right) + \mathcal{O}(\epsilon^3) \right]. \quad (5)$$

Let  $B_3$  denote the sum of all the three-loop diagrams from Table I, after performing the above replacement. Our final result for  $G_{77}(0, \mu)$  is found according to the following formula

$$G_{77}(0, \mu) = \frac{1}{16} \left( Z_m^{\overline{\text{MS}}} Z_{77}^{\overline{\text{MS}}} \right)^2 Z_\psi^{\text{OS}} \left[ B_1 + \frac{\alpha_s(\mu)}{4\pi} Z_\alpha^{\overline{\text{MS}}} \frac{\mu^{2\epsilon}}{m_b^{2\epsilon}} (B_2 + (Z_m^{\text{OS}} - 1) B_2^m) + \left( \frac{\alpha_s}{4\pi} \right)^2 \frac{\mu^{4\epsilon}}{m_b^{4\epsilon}} B_3 \right] + \mathcal{O}(\alpha_s^3), \quad (6)$$

where

$$B_1 = 16 + 16\epsilon + \left( 32 - \frac{16}{3}\pi^2 \right) \epsilon^2 + \mathcal{O}(\epsilon^3), \quad (7)$$

$$B_2 = C_F \left[ \frac{16}{\epsilon} + \frac{496}{3} - \frac{64}{3}\pi^2 + \epsilon (848 - 80\pi^2 - 256\zeta_3) + \mathcal{O}(\epsilon^2) \right] \quad (8)$$

stand for the one-loop (Born) diagram and the sum of two-loop diagrams, respectively. The  $\overline{\text{MS}}$  renormalization constant for the operator vertex

$$Z_m^{\overline{\text{MS}}} Z_{77}^{\overline{\text{MS}}} = 1 + \frac{\alpha_s(\mu)}{4\pi} \frac{C_F}{\epsilon} + \left( \frac{\alpha_s}{4\pi} \right)^2 \frac{C_F}{\epsilon} \left[ \frac{257}{36} C_A - \frac{19}{4} C_F - \frac{13}{9} T_R N_f + \frac{1}{\epsilon} \left( \frac{1}{2} C_F - \frac{11}{6} C_A + \frac{2}{3} T_R N_f \right) \right] + \mathcal{O}(\alpha_s^3) \quad (9)$$

is found from the anomalous dimensions published in Ref. [26]. The on-shell renormalization constant of the quark field can be written as [27]

$$Z_\psi^{\text{OS}} = 1 + \left( \frac{\alpha_s(\mu)}{4\pi} \right) P_1 + \left( \frac{\alpha_s}{4\pi} \right)^2 P_2 + \mathcal{O}(\alpha_s^3), \quad (10)$$

where

$$P_1 = C_F \left[ -\frac{3}{\epsilon} - 4 + 6 \ln \frac{m_b}{\mu} + \epsilon \left( -8 + 8 \ln \frac{m_b}{\mu} - 6 \ln^2 \frac{m_b}{\mu} \right) + \mathcal{O}(\epsilon^2) \right], \quad (11)$$

$$P_2 = C_F (T_R N_L P_L + T_R N_H P_H + C_F P_A + C_A P_{NA}), \quad (12)$$

and

$$P_L = -\frac{2}{\epsilon^2} + \frac{11}{3\epsilon} + \frac{113}{6} + \frac{4}{3} \pi^2 - \frac{76}{3} \ln \frac{m_b}{\mu} + 8 \ln^2 \frac{m_b}{\mu} + \mathcal{O}(\epsilon), \quad (13)$$

$$P_H = \frac{1}{\epsilon} - \frac{8}{\epsilon} \ln \frac{m_b}{\mu} + \frac{947}{18} - \frac{16}{3} \pi^2 - \frac{44}{3} \ln \frac{m_b}{\mu} + 24 \ln^2 \frac{m_b}{\mu} + \mathcal{O}(\epsilon), \quad (14)$$

$$P_{NA} = \frac{11}{2\epsilon^2} - \frac{127}{12\epsilon} - \frac{1705}{24} + 5\pi^2 - 8\pi^2 \ln 2 + 12\zeta_3 + \frac{215}{3} \ln \frac{m_b}{\mu} - 22 \ln^2 \frac{m_b}{\mu} + \mathcal{O}(\epsilon), \quad (15)$$

$$P_A = \frac{9}{2\epsilon^2} + \frac{1}{\epsilon} \left( \frac{51}{4} - 18 \ln \frac{m_b}{\mu} \right) + \frac{433}{8} - 13\pi^2 + 16\pi^2 \ln 2 - 24\zeta_3 - 51 \ln \frac{m_b}{\mu} + 36 \ln^2 \frac{m_b}{\mu} + \mathcal{O}(\epsilon). \quad (16)$$

Mass renormalization in the  $b$  quark propagators is accounted for by squaring these propagators in the two-loop diagrams, which turns  $B_2$  into

$$B_2^m = C_F \left[ \frac{1}{\epsilon} (96 - 48\xi) + 656 - 16\xi - 64\pi^2 + \epsilon (2344 - 256\xi - 160\pi^2 + 16\pi^2\xi - 768\zeta_3) \right]. \quad (17)$$

In the expression (6) for  $G_{77}$ , the above quantity gets multiplied by  $Z_m^{\text{OS}} - 1 = \frac{\alpha_s}{4\pi} P_1 + \mathcal{O}(\alpha_s^2)$ . For completeness, the one-loop gauge coupling renormalization constant should also be mentioned

$$Z_\alpha^{\overline{\text{MS}}} = 1 + \left( \frac{\alpha_s}{4\pi} \right) \left( \frac{4}{3} T_R N_f - \frac{11}{3} C_A \right) + \mathcal{O}(\alpha_s^2). \quad (18)$$

### III. RESULTS

Our final results for the contributions to  $G_{77}(0, \mu)$  read

$$\begin{aligned} X_1 &= C_F \left( \frac{16}{3} + 4 \ln \frac{m_b}{\mu} - \frac{4}{3} \pi^2 \right), \\ X_L &= -\frac{251}{27} + \left( -\frac{32}{9} \pi^2 + \frac{8}{3} \right) \ln \frac{m_b}{\mu} + \frac{16}{3} \ln^2 \frac{m_b}{\mu} + 16\zeta_3 + \frac{128}{27} \pi^2, \\ X_H &= \frac{7126}{81} + \left( -\frac{32}{9} \pi^2 + \frac{8}{3} \right) \ln \frac{m_b}{\mu} + \frac{16}{3} \ln^2 \frac{m_b}{\mu} - \frac{16}{3} \zeta_3 - \frac{232}{27} \pi^2, \\ X_{NA} &= -\frac{1333}{216} + \left( \frac{88}{9} \pi^2 + 18 \right) \ln \frac{m_b}{\mu} - \frac{44}{3} \ln^2 \frac{m_b}{\mu} - \frac{47}{6} \zeta_3 - 27\pi^2 \ln 2 + \frac{119}{108} \pi^2 + \frac{43}{90} \pi^4, \\ X_A &= \frac{2825}{18} - \left( \frac{16}{3} \pi^2 + \frac{50}{3} \right) \ln \frac{m_b}{\mu} + 8 \ln^2 \frac{m_b}{\mu} - \frac{217}{3} \zeta_3 + 54\pi^2 \ln 2 - \frac{319}{6} \pi^2 + \frac{53}{45} \pi^4. \end{aligned} \quad (19)$$

The complete (logarithmic and constant) contribution of the light quark loops has already been found in Ref. [19]. However, the decay width was normalized there with  $m_b^5$  rather than with  $m_b(\mu)^2 m_b^3$  as in Eq. (1) here. In order to compare with that study, we multiply our result for  $G_{77}$  by  $m_b^2(\mu)/m_b^2$ . In other words, we write

$$\Gamma(b \rightarrow X_s^{\text{parton}} \gamma)_{E_\gamma > E_0} = \frac{G_F^2 \alpha_{\text{em}} m_b^5}{32\pi^4} |V_{tb} V_{ts}^*|^2 \sum_{i,j} C_i^{\text{eff}}(\mu) C_j^{\text{eff}}(\mu) \tilde{G}_{ij}(E_0, \mu), \quad (20)$$

where

$$\tilde{G}_{77}(0, \mu) = 1 + \left( \frac{\alpha_s(\mu)}{4\pi} \right) \tilde{X}_1 + \left( \frac{\alpha_s}{4\pi} \right)^2 \tilde{X}_2 + \mathcal{O}(\alpha_s^3). \quad (21)$$

and

$$\tilde{X}_2 = C_F \left( T_R N_L \tilde{X}_L + T_R N_H \tilde{X}_H + C_F \tilde{X}_A + C_A \tilde{X}_{NA} \right). \quad (22)$$

The connection between the pole-mass  $m_b$  and the  $\overline{\text{MS}}$  mass  $m_b(\mu)$  is now known to the three-loop order [28]. Here, we only need it to two-loops [29]

$$\begin{aligned} \frac{m_b(\mu)}{m_b} = & 1 + C_F \frac{\alpha_s(\mu)}{4\pi} \left( -4 + 6 \ln \frac{m_b}{\mu} \right) + C_F \left( \frac{\alpha_s}{4\pi} \right)^2 \left[ T_R N_L \left( \frac{71}{6} + \frac{4}{3} \pi^2 - \frac{52}{3} \ln \frac{m_b}{\mu} + 8 \ln^2 \frac{m_b}{\mu} \right) \right. \\ & + T_R N_H \left( \frac{143}{6} - \frac{8}{3} \pi^2 - \frac{52}{3} \ln \frac{m_b}{\mu} + 8 \ln^2 \frac{m_b}{\mu} \right) \\ & + C_F \left( \frac{7}{8} + 8 \pi^2 \ln 2 - 5 \pi^2 - 12 \zeta_3 - 21 \ln \frac{m_b}{\mu} + 18 \ln^2 \frac{m_b}{\mu} \right) \\ & \left. + C_A \left( -\frac{1111}{24} - 4 \pi^2 \ln 2 + \frac{4}{3} \pi^2 + 6 \zeta_3 + \frac{185}{3} \ln \frac{m_b}{\mu} - 22 \ln^2 \frac{m_b}{\mu} \right) \right]. \quad (23) \end{aligned}$$

Using the above relation, we obtain

$$\begin{aligned} \tilde{X}_1 &= C_F \left( -\frac{8}{3} + 16 \ln \frac{m_b}{\mu} - \frac{4}{3} \pi^2 \right), \\ \tilde{X}_L &= \frac{388}{27} - \left( \frac{32}{9} \pi^2 + 32 \right) \ln \frac{m_b}{\mu} + \frac{64}{3} \ln^2 \frac{m_b}{\mu} + 16 \zeta_3 + \frac{200}{27} \pi^2, \\ \tilde{X}_H &= \frac{10987}{81} - \left( \frac{32}{9} \pi^2 + 32 \right) \ln \frac{m_b}{\mu} + \frac{64}{3} \ln^2 \frac{m_b}{\mu} - \frac{16}{3} \zeta_3 - \frac{376}{27} \pi^2, \\ \tilde{X}_{NA} &= -\frac{21331}{216} + \left( \frac{88}{9} \pi^2 + \frac{424}{3} \right) \ln \frac{m_b}{\mu} - \frac{176}{3} \ln^2 \frac{m_b}{\mu} + \frac{25}{6} \zeta_3 - 35 \pi^2 \ln 2 + \frac{407}{108} \pi^2 + \frac{43}{90} \pi^4, \\ \tilde{X}_A &= \frac{4753}{36} - \left( \frac{64}{3} \pi^2 + \frac{224}{3} \right) \ln \frac{m_b}{\mu} + 128 \ln^2 \frac{m_b}{\mu} - \frac{289}{3} \zeta_3 + 70 \pi^2 \ln 2 - \frac{105}{2} \pi^2 + \frac{53}{45} \pi^4. \quad (24) \end{aligned}$$

We find complete agreement of the  $\tilde{X}_L$  result with Ref. [19]. In that work, along the hypothesis of naive non-abelianization (NNA),  $\tilde{X}_L$  was multiplied by  $-3/2 \beta_0(N_f = 5)$  in order to estimate  $\tilde{X}_2$ . Our complete result for  $\tilde{X}_2$  allows us to check this hypothesis. Including all the SU(3) color factors, our analytic result leads to (for  $N_L = 4$  and  $N_H = 1$ )

$$(\tilde{X}_2)_{\text{exact}} \simeq -555.7 + 220.7 \ln \frac{m_b}{\mu} + 64.0 \ln^2 \frac{m_b}{\mu}, \quad (25)$$

$$(\tilde{X}_2)_{\text{NNA}} \equiv C_F T_R (-3\beta_0/2) \tilde{X}_L \simeq -818.1 + 514.4 \ln \frac{m_b}{\mu} - 163.6 \ln^2 \frac{m_b}{\mu}. \quad (26)$$

Evidently, there are substantial differences between these expressions, from which we conclude that the NNA hypothesis does not necessarily improve on the  $\tilde{X}_L$  component of the  $\mathcal{O}(\alpha_s^2)$  part of the calculation.

The large numerical value of the NNLO correction coefficient in Eq. (25) may be traced back to the infrared sensitivity of the pole mass  $m_b$  whose fifth power stands in front of the expression (20) for the decay rate. Following Ref. [30], we shall normalize the  $b \rightarrow X_s^{\text{parton}} \gamma$  rate to the semileptonic rate

$$\Gamma(b \rightarrow X_u^{\text{parton}} e \bar{\nu}) = \frac{G_F^2 m_b^5}{192\pi^3} |V_{ub}|^2 G_u. \quad (27)$$

From the results Ref. [31], one finds

$$G_u \simeq 1 - 9.65 \left( \frac{\alpha_s(\mu)}{4\pi} \right) + \left( \frac{\alpha_s}{4\pi} \right)^2 \left[ -340.7 + 148.0 \ln \frac{m_b}{\mu} \right] + \mathcal{O}(\alpha_s^3), \quad (28)$$

$$(G_u)_{\text{NNA}} \simeq 1 - 9.65 \left( \frac{\alpha_s(\mu)}{4\pi} \right) + \left( \frac{\alpha_s}{4\pi} \right)^2 \left[ -395.0 + 148.0 \ln \frac{m_b}{\mu} \right] + \mathcal{O}(\alpha_s^3). \quad (29)$$

Dividing our results by  $\Gamma(b \rightarrow X_u^{\text{parton}} e \bar{\nu})$  and expanding up to  $\mathcal{O}(\alpha_s^2)$ , we obtain

$$\frac{\pi}{6\alpha_{\text{em}}} \left| \frac{V_{ub}}{V_{tb}V_{ts}^*} \right|^2 \frac{\Gamma(b \rightarrow X_s^{\text{parton}} \gamma)_{E_\gamma > E_0}}{\Gamma(b \rightarrow X_u^{\text{parton}} e \bar{\nu})} = \sum_{i,j} C_i^{\text{eff}}(\mu) C_j^{\text{eff}}(\mu) \frac{\tilde{G}_{ij}(E_0, \mu)}{G_u} = \frac{m_b^2(\mu)}{m_b^2} \sum_{i,j} C_i^{\text{eff}}(\mu) C_j^{\text{eff}}(\mu) \frac{G_{ij}(E_0, \mu)}{G_u}, \quad (30)$$

and

$$\begin{aligned} \frac{\tilde{G}_{77}(0, \mu)}{G_u} &\simeq 1 + \left( \frac{\alpha_s(\mu)}{4\pi} \right) \left[ -11.45 + 21.33 \ln \frac{m_b^{\text{pole}}}{\mu} \right] + \left( \frac{\alpha_s}{4\pi} \right)^2 \left[ -325.5 + 278.6 \ln \frac{m_b}{\mu} + 64.0 \ln^2 \frac{m_b}{\mu} \right] \\ &\simeq 1 + \left( \frac{\alpha_s(\mu)}{4\pi} \right) \left[ -11.45 + 21.33 \ln \frac{m_b(\mu)}{\mu} \right] + \left( \frac{\alpha_s}{4\pi} \right)^2 \left[ -211.7 + 107.9 \ln \frac{m_b}{\mu} + 64.0 \ln^2 \frac{m_b}{\mu} \right], \end{aligned} \quad (31)$$

$$\left( \frac{\tilde{G}_{77}}{G_u} \right)_{\text{NNA}} \simeq 1 + \left( \frac{\alpha_s(\mu)}{4\pi} \right) \left[ -11.45 + 21.33 \ln \frac{m_b}{\mu} \right] + \left( \frac{\alpha_s}{4\pi} \right)^2 \left[ -423.1 + 366.4 \ln \frac{m_b}{\mu} - 163.6 \ln^2 \frac{m_b}{\mu} \right], \quad (32)$$

$$\begin{aligned} \frac{G_{77}(0, \mu)}{G_u} &\simeq 1 + \left( \frac{\alpha_s(\mu)}{4\pi} \right) \left[ -0.78 + 5.33 \ln \frac{m_b^{\text{pole}}}{\mu} \right] + \left( \frac{\alpha_s}{4\pi} \right)^2 \left[ -37.0 + 130.2 \ln \frac{m_b}{\mu} - 26.7 \ln^2 \frac{m_b}{\mu} \right] \\ &\simeq 1 + \left( \frac{\alpha_s(\mu)}{4\pi} \right) \left[ -0.78 + 5.33 \ln \frac{m_b(\mu)}{\mu} \right] + \left( \frac{\alpha_s}{4\pi} \right)^2 \left[ -8.5 + 87.5 \ln \frac{m_b}{\mu} - 26.7 \ln^2 \frac{m_b}{\mu} \right], \end{aligned} \quad (33)$$

$$\left( \frac{G_{77}}{G_u} \right)_{\text{NNA}} \simeq 1 + \left( \frac{\alpha_s(\mu)}{4\pi} \right) \left[ -0.78 + 5.33 \ln \frac{m_b}{\mu} \right] + \left( \frac{\alpha_s}{4\pi} \right)^2 \left[ -39.9 + 100.6 \ln \frac{m_b}{\mu} - 40.9 \ln^2 \frac{m_b}{\mu} \right]. \quad (34)$$

Note that  $(G_{77}/G_u)_{\text{NNA}}$  differs from  $(G_{77})_{\text{NNA}}/(G_u)_{\text{NNA}}$ . The latter quantity gives a worse approximation to the complete result. The same is true for  $\tilde{G}_{77}$ .

In order to indicate where the renormalization of  $m_b$  matters in the above expressions, we have introduced the superscript “pole” for the pole mass. Actually, no renormalization of  $m_b$  needs to be performed when evaluating the  $\mathcal{O}(\alpha_s^2)$  terms in the NNA approach. However, it is mandatory to identify the mass in this approach with the pole mass because it often originates from the square of the external momentum.

Comparing the  $\mu$ -independent terms in Eqs. (31)–(34) one concludes that the perturbation series converges much better and the NNA gives a better approximation for  $G_{77}/G_u$  rather than for  $\tilde{G}_{77}/G_u$ . This observation confirms that the normalization of the top quark contribution to the  $b \rightarrow s \gamma$  amplitude which was applied at the NLO in Ref. [30] indeed helped in reducing the NNLO contributions that were unknown at that time. As far as the charm-sector amplitude is concerned, no conclusion can be drawn yet, because several important NNLO ingredients are still missing.

We have checked that the  $\mu$ -dependent terms in the complete (i.e., non-NNA) expressions for  $\tilde{G}_{77}(0, \mu) = G_{77}(0, \mu) m_b^2(\mu)/m_b^2$  cancel out (analytically) with the corresponding ones that originate from the Wilson coefficient

$$C_7^{\text{eff}}(\mu) = C_7^{(0)\text{eff}}(\mu) + \left( \frac{\alpha_s(\mu)}{4\pi} \right) C_7^{(1)\text{eff}}(\mu) + \left( \frac{\alpha_s}{4\pi} \right)^2 C_7^{(2)\text{eff}}(\mu) + \mathcal{O}(\alpha_s^3). \quad (35)$$

Of course, it does not mean that the quantity  $(C_7^{\text{eff}}(\mu))^2 \tilde{G}_{77}(0, \mu)$  is  $\mu$ -independent at  $\mathcal{O}(\alpha_s^2)$  — other operators need to be included for a complete cancellation, for instance,

$$O_8 = \frac{gm_b(\mu)}{16\pi^2} \bar{s}_L \sigma^{\mu\nu} T^a b_R G_{\mu\nu}^a. \quad (36)$$

As far as the  $\mu$ -independent terms in the Wilson coefficients are concerned, we can check their values for the top-sector amplitude, for which all the relevant Wilson coefficients are now available at the NNLO [13, 14, 15]. In

particular, setting the matching scale  $\mu_0$  to  $m_t(m_t)$  and the low-energy scale  $\mu$  to  $m_b(m_b)$ , we find

$$C_7^{t\text{ eff}}(m_b(m_b)) = C_7^{t(0)\text{ eff}}(m_b(m_b)) \left[ 1 - 7.25 \left( \frac{\alpha_s(m_b)}{4\pi} \right) + 17.7 \left( \frac{\alpha_s(m_b)}{4\pi} \right)^2 + \mathcal{O}(\alpha_s^3) \right], \quad (37)$$

$$C_8^{t\text{ eff}}(m_b(m_b)) = C_8^{t(0)\text{ eff}}(m_b(m_b)) \left[ 1 - 5.21 \left( \frac{\alpha_s(m_b)}{4\pi} \right) + 38.7 \left( \frac{\alpha_s(m_b)}{4\pi} \right)^2 + \mathcal{O}(\alpha_s^3) \right]. \quad (38)$$

Thus, no large corrections to the Wilson coefficients are being observed, which means that the NNLO QCD corrections to  $(C_7^{t\text{ eff}})^2 G_{77}/G_u$  are significantly smaller than to  $(C_7^{t\text{ eff}})^2 \tilde{G}_{77}/G_u$ .

Among the dipole operator contributions, there are still missing two-loop matrix elements of  $O_8$  and the  $\mathcal{O}(\alpha_s^2)$  corrections to the interference of amplitudes arising from  $O_7$  and  $O_8$ . The set of master integrals in the form available so far [24] is not sufficient for those calculations. The reason is that the imaginary parts of those integrals are presented as sums over all cuts, while in the case of  $O_8$  we sometimes have cuts which do not correspond to the decay  $b \rightarrow s\gamma$ . Thus, it would be desirable to recalculate the master integrals in such a way that each individual cut contribution is known separately. If that were done, one could apply the same algebraic reduction of all integrals to the set of master integrals, keeping track of the relevant cuts. This would give an analytic result for  $G_{78}(0, \mu)$ . A calculation of  $G_{88}(E_0, \mu)$  would be much more difficult because of the IR divergences at  $E_0 \rightarrow 0$  and collinear divergences at  $m_s \rightarrow 0$ . Fortunately, the effect of  $G_{88}$  on the decay rate is suppressed by the square of the down quark charge or, more precisely, by  $(Q_d C_8/C_7)^2 \sim 0.03$ . Consequently, the  $\mathcal{O}(\alpha_s^2)$  corrections to  $G_{88}(E_0, \mu)$  are negligible.

#### IV. CONCLUSIONS

We have evaluated two-loop QCD corrections to the matrix element of  $O_7$  together with the corresponding bremsstrahlung contributions. The size of the resulting (partial)  $\mathcal{O}(\alpha_s^2)$  correction to  $\Gamma(\bar{B} \rightarrow X_s \gamma)/\Gamma(\bar{B} \rightarrow X_u e \bar{\nu})$  depends very much on the conventions for the factors of  $m_b$  that normalize the decay rates. When both of them are normalized to  $m_{b,R}^5$  in the same renormalization scheme  $R$ , the  $\mathcal{O}(\alpha_s^2)$  correction is sizeable ( $\sim 6\%$ ), and the NNA estimate is about 1/3 too large. On the other hand, when the ratio of the decay widths is written as  $S \times m_{b,\overline{\text{MS}}}^2(m_b)/m_{b,\text{pole}}^2$ , the calculated  $\mathcal{O}(\alpha_s^2)$  correction to  $S$  is at the level of 1% for both the complete and the NNA results.

#### V. ACKNOWLEDGMENTS

A. C. gratefully acknowledges very helpful correspondence with Matthias Steinhauser. M. M. would like to thank Ulrich Haisch for verifying the NNLO corrections to the Wilson coefficients. I. B. and A. C. were supported by Science and Engineering Research Canada. M. M. was supported in part by the Polish Committee for Scientific Research under the grant 2 P03B 078 26, and from the European Community's Human Potential Programme under the contract HPRN-CT-2002-00311, EURIDICE. M. Š. was supported by the Alberta Ingenuity Postdoctoral Fellowship.



- 
- [1] M. A. Shifman, A. I. Vainshtein and V. I. Zakharov, Sov. Phys. JETP **45**, 670 (1977) [Zh. Eksp. Teor. Fiz. **72**, 1275 (1977)].
  - [2] P. Gambino, U. Haisch and M. Misiak, Phys. Rev. Lett. **94**, 061803 (2005) [hep-ph/0410155].
  - [3] J. Alexander *et al.* (Heavy Flavor Averaging Group), hep-ex/0412073.
  - [4] A. Czarnecki and W.J. Marciano, Phys. Rev. Lett. **81** 277, (1998) [hep-ph/9804252].
  - [5] A. Strumia, Nucl. Phys. B **532**, 28 (1998) [hep-ph/9804274].
  - [6] A.L. Kagan and M. Neubert, Eur. Phys. J. C **7**, 5 (1999) [hep-ph/9805303].
  - [7] K. Baranowski and M. Misiak, Phys. Lett. B **483**, 410 (2000) [hep-ph/9907427].
  - [8] P. Gambino and U. Haisch, JHEP **09**, 001 (2000) [hep-ph/0007259]; JHEP **10**, 020 (2001) [hep-ph/0109058].
  - [9] A.J. Buras, A. Czarnecki, M. Misiak and J. Urban, Nucl. Phys. B **631**, 219 (2002) [hep-ph/0203135].
  - [10] A. J. Buras and M. Misiak, Acta Phys. Polon. B **33**, 2597 (2002) [hep-ph/0207131].
  - [11] A.F. Falk, M.E. Luke and M.J. Savage, Phys. Rev. D **49**, 3367 (1994) [hep-ph/9308288];  
G. Buchalla, G. Isidori and S.J. Rey, Nucl. Phys. B **511**, 594 (1998) [hep-ph/9705253];  
M. Neubert, Eur. Phys. J. C **40**, 165 (2005) [hep-ph/0408179].
  - [12] M. Misiak, Acta Phys. Polon. B **34**, 4397 (2003).
  - [13] M. Gorbahn and U. Haisch, Nucl. Phys. B **713**, 291 (2005) [hep-ph/0411071].
  - [14] M. Gorbahn, U. Haisch and M. Misiak, hep-ph/0504194.
  - [15] M. Misiak and M. Steinhauser, Nucl. Phys. B **683**, 277 (2004) [hep-ph/0401041].
  - [16] H. M. Asatrian, C. Greub, A. Hovhannisyan, T. Hurth and V. Poghosyan, hep-ph/0505068.
  - [17] C. Greub, T. Hurth and D. Wyler, Phys. Rev. D **54**, 3350 (1996) [hep-ph/9603404].
  - [18] A. J. Buras, A. Czarnecki, M. Misiak and J. Urban, Nucl. Phys. B **611**, 488 (2001) [hep-ph/0105160].
  - [19] K. Bieri, C. Greub and M. Steinhauser, Phys. Rev. D **67**, 114019 (2003) [hep-ph/0302051].
  - [20] A.J. Buras, M. Misiak, M. Münz and S. Pokorski, Nucl. Phys. B **424**, 374 (1994) [hep-ph/9311345].
  - [21] K. Melnikov and A. Mitov, hep-ph/0505097.
  - [22] A. Ali and C. Greub, Z. Phys. C **49**, 431 (1991), Phys. Lett. B **259**, 182 (1991), Phys. Lett. B **361**, 146 (1995) [hep-ph/9506374].
  - [23] I. Blokland, A. Czarnecki, M. Ślusarczyk and F. Tkachov, Phys. Rev. Lett. **93**, 062001 (2004) [hep-ph/0403221].
  - [24] I. Blokland, A. Czarnecki, M. Ślusarczyk and F. Tkachov, Phys. Rev. D **71**, 054004 (2005) [hep-ph/0503039].
  - [25] T. Muta, *Foundations Of Quantum Chromodynamics*, World Sci. Lect. Notes Phys. **5**, 1 (1987).
  - [26] M. Misiak and M. Münz, Phys. Lett. B **344**, 308 (1995) [hep-ph/9409454].
  - [27] D. J. Broadhurst, N. Gray and K. Schilcher, Z. Phys. C **52**, 111 (1991).
  - [28] K. G. Chetyrkin and M. Steinhauser, Phys. Rev. Lett. **83**, 4001 (1999) [hep-ph/9907509]; Nucl. Phys. B **573**, 617 (2000) [hep-ph/9911434];  
K. Melnikov and T. v. Ritbergen, Phys. Lett. B **482**, 99 (2000) [hep-ph/9912391].
  - [29] N. Gray, D. J. Broadhurst, W. Grafe and K. Schilcher, Z. Phys. C **48**, 673 (1990).
  - [30] P. Gambino and M. Misiak, Nucl. Phys. B **611**, 338 (2001) [hep-ph/0104034].
  - [31] T. van Ritbergen, Phys. Lett. B **454**, 353 (1999) [hep-ph/9903226].



## APPENDIX A: RESULTS FOR PARTICULAR DIAGRAMS

Diagram	Color factor	
(a)	$C_F^2$	$\frac{1}{\epsilon^2} [32 - 32\xi + 8\xi^2] + \frac{1}{\epsilon} [\frac{1264}{3} - \frac{1048}{3}\xi + \frac{208}{3}\xi^2] + \frac{29632}{9} - 32\pi^2\xi - 16\pi^2\xi^2 - 40\pi^2 - \frac{14884}{9}\xi + \frac{4156}{9}\xi^2$
(b)	$C_F (C_F - \frac{C_A}{2})$	$-92 + 192\zeta_3\xi + \frac{208}{3}\zeta_3 - 48\pi^2\xi + \frac{224}{3}\pi^2 \ln 2 - 8\pi^2 - \frac{112}{45}\pi^4 + 96\xi + 16\xi^2$
(c)	$C_F (C_F - \frac{C_A}{2})$	$\frac{1}{\epsilon^2} [16\xi + 16\xi^2] + \frac{1}{\epsilon} [64 - \frac{64}{3}\pi^2\xi - \frac{64}{3}\pi^2 + \frac{416}{3}\xi + \frac{320}{3}\xi^2] + \frac{1792}{3} - 448\zeta_3\xi - 448\zeta_3 - \frac{272}{3}\pi^2\xi - 32\pi^2\xi^2 - 144\pi^2 + \frac{128}{15}\pi^4 + \frac{7184}{9}\xi + \frac{4880}{9}\xi^2$
(d)	$C_F (C_F - \frac{C_A}{2})$	$\frac{1}{\epsilon^2} [-16 - 32\xi - 16\xi^2] + \frac{1}{\epsilon} [-\frac{296}{3} - \frac{664}{3}\xi - \frac{332}{3}\xi^2] - \frac{4724}{9} + 64\pi^2\xi + 32\pi^2\xi^2 + 32\pi^2 - \frac{10636}{9}\xi - \frac{5318}{9}\xi^2$
(e)	$C_F^2$	$\frac{1}{\epsilon^2} [16\xi^2] + \frac{1}{\epsilon} [-\frac{64}{3}\pi^2\xi + 32\xi + \frac{320}{3}\xi^2] + 128 - 256\zeta_3\xi - \frac{320}{3}\pi^2\xi - 32\pi^2\xi^2 - \frac{64}{3}\pi^2 + \frac{64}{15}\pi^4 + 272\xi + \frac{5024}{9}\xi^2$
(f)	$C_F (C_F - \frac{C_A}{2})$	$\frac{1}{\epsilon} [-64 + 64\xi - 16\xi^2] + \frac{248}{9} - 512\zeta_3 + 96\pi^2\xi - \frac{112}{3}\pi^2 - \frac{376}{3}\xi - \frac{524}{3}\xi^2$
(g)	$C_F^2$	$\frac{1}{\epsilon^2} [16 + 32\xi + 16\xi^2] + \frac{1}{\epsilon} [\frac{320}{3} + \frac{640}{3}\xi + \frac{320}{3}\xi^2] + \frac{5024}{9} - 64\pi^2\xi - 32\pi^2\xi^2 - 32\pi^2 + \frac{10048}{9}\xi + \frac{5024}{9}\xi^2$
(h)	$C_F^2$	$\frac{1}{\epsilon^2} [8 + 16\xi + 8\xi^2] + \frac{1}{\epsilon} [\frac{172}{3} + \frac{344}{3}\xi + \frac{172}{3}\xi^2] + \frac{2878}{9} - 32\pi^2\xi - 16\pi^2\xi^2 - 16\pi^2 + \frac{5756}{9}\xi + \frac{2878}{9}\xi^2$
(i)	$C_F^2$	$\frac{1}{\epsilon^2} [-32 - 16\xi + 16\xi^2] + \frac{1}{\epsilon} [-\frac{856}{3} - \frac{536}{3}\xi + \frac{320}{3}\xi^2] - \frac{16012}{9} + 32\pi^2\xi - 32\pi^2\xi^2 + 64\pi^2 - \frac{10844}{9}\xi + \frac{5168}{9}\xi^2$
(j)	$C_F^2$	$\frac{1}{\epsilon^2} [64\xi - 32\xi^2] + \frac{1}{\epsilon} [64 + \frac{64}{3}\pi^2\xi - \frac{128}{3}\pi^2 + \frac{1616}{3}\xi - \frac{640}{3}\xi^2] + 832 + 640\zeta_3\xi - 1280\zeta_3 + \frac{80}{3}\pi^2\xi + 48\pi^2\xi^2 - \frac{896}{3}\pi^2 + \frac{26840}{9}\xi - \frac{10192}{9}\xi^2$
(k)	$C_F (C_F - \frac{C_A}{2})$	$-560 - 576\zeta_3\xi + 2304\zeta_3 + 16\pi^2\xi^2 - \frac{592}{3}\pi^2 + \frac{64}{45}\pi^4 + 208\xi - 16\xi^2$
(l)	$C_F^2$	$\frac{1}{\epsilon^2} [-16\xi - 16\xi^2] + \frac{1}{\epsilon} [-32 + \frac{64}{3}\pi^2\xi + \frac{64}{3}\pi^2 - \frac{416}{3}\xi - \frac{320}{3}\xi^2] - 352 + 256\zeta_3\xi + 256\zeta_3 + \frac{416}{3}\pi^2\xi + 32\pi^2\xi^2 + \frac{320}{3}\pi^2 - \frac{8336}{9}\xi - \frac{5168}{9}\xi^2$
(m)	$C_F^2$	$\frac{1}{\epsilon^2} [-32\xi - 32\xi^2] + \frac{1}{\epsilon} [-32 + \frac{64}{3}\pi^2\xi + \frac{64}{3}\pi^2 - \frac{736}{3}\xi - \frac{640}{3}\xi^2] - 272 + 256\zeta_3\xi + 256\zeta_3 + \frac{512}{3}\pi^2\xi + 64\pi^2\xi^2 + \frac{320}{3}\pi^2 - \frac{12496}{9}\xi - \frac{10048}{9}\xi^2$
(n)	$C_F^2$	$\frac{1}{\epsilon^2} [16\xi^2] + \frac{1}{\epsilon} [-\frac{64}{3}\pi^2\xi + 32\xi + \frac{272}{3}\xi^2] - 128 - 256\zeta_3\xi - \frac{320}{3}\pi^2\xi - \frac{80}{3}\pi^2\xi^2 + \frac{128}{3}\pi^2 - \frac{64}{45}\pi^4 + 368\xi + \frac{3920}{9}\xi^2$
(o)	$C_F (C_F - \frac{C_A}{2})$	$\frac{1}{\epsilon} [64 + 16\xi^2] + \frac{4360}{3} + 192\zeta_3\xi - \frac{800}{3}\zeta_3 - 48\pi^2\xi - \frac{16}{3}\pi^2\xi^2 + \frac{448}{3}\pi^2 \ln 2 - 224\pi^2 + \frac{224}{45}\pi^4 + \frac{416}{3}\xi^2$

TABLE I: Imaginary parts of three-loop self-energy diagrams in a general covariant gauge.

Topology	Color factor	
(p)	$C_F^2$	$\frac{1}{\epsilon^2} [736 - 400\xi + 16\xi^2] + \frac{1}{\epsilon} \left[ \frac{8672}{3} - \frac{3248}{3}\xi + \frac{320}{3}\xi^2 \right] + \frac{136640}{9} + 400\pi^2\xi - 16\pi^2\xi^2 - 736\pi^2 - \frac{62528}{9}\xi + \frac{5024}{9}\xi^2$
(q)	$C_F (C_F - \frac{C_A}{2})$	$\frac{1}{\epsilon^2} [128 - 32\xi - 16\xi^2] + \frac{1}{\epsilon} \left[ \frac{2128}{3} + \frac{224}{3}\xi - \frac{320}{3}\xi^2 \right] + \frac{14264}{3} - 2048\zeta_3 + 32\pi^2\xi + 16\pi^2\xi^2 - 128\pi^2 + \frac{12416}{9}\xi - \frac{5024}{9}\xi^2$
(r)	$C_F^2$	$\frac{1}{\epsilon^2} [-576 + 272\xi - 16\xi^2] + \frac{1}{\epsilon} \left[ -1280 + \frac{64}{3}\pi^2\xi - \frac{512}{3}\pi^2 + \frac{1888}{3}\xi - \frac{320}{3}\xi^2 \right] - 7184 + 256\zeta_3\xi - 2048\zeta_3 - \frac{592}{3}\pi^2\xi + 16\pi^2\xi^2 + \frac{320}{3}\pi^2 + \frac{35296}{9}\xi - \frac{5024}{9}\xi^2$
(s)	$C_F (C_F - \frac{C_A}{2})$	$\frac{1}{\epsilon^2} [16\xi + 16\xi^2] + \frac{1}{\epsilon} \left[ 64 - \frac{64}{3}\pi^2\xi - \frac{64}{3}\pi^2 + \frac{416}{3}\xi + \frac{320}{3}\xi^2 \right] - \frac{20080}{9} - 256\zeta_3\xi + 384\zeta_3 - \frac{560}{3}\pi^2\xi - 16\pi^2\xi^2 + 384\pi^2 \ln 2 - \frac{352}{3}\pi^2 + \frac{32}{9}\pi^4 + \frac{3872}{9}\xi + \frac{5024}{9}\xi^2$
(t)	$-\frac{1}{2}C_FC_A$	$\frac{1}{\epsilon^2} [-48\xi - 24\xi^2] + \frac{1}{\epsilon} \left[ -96 + 32\pi^2\xi + 64\pi^2 - 432\xi - 176\xi^2 \right] - 1040 + 672\zeta_3\xi + 768\zeta_3 + 256\pi^2\xi + \frac{64}{3}\pi^2\xi^2 + \frac{1160}{3}\pi^2 - \frac{352}{45}\pi^4 - \frac{6520}{3}\xi - 968\xi^2$
(u)	$-\frac{1}{2}C_FC_A$	$272 + 288\zeta_3\xi - 192\zeta_3 + \frac{64}{3}\pi^2\xi - 16\pi^2\xi^2 + 88\pi^2 - \frac{352}{45}\pi^4 - 320\xi$
(v)	$-\frac{1}{2}C_FC_A$	$\frac{1}{\epsilon^2} [-192 + 48\xi + 24\xi^2] + \frac{1}{\epsilon} [-1424 - 8\xi + 192\xi^2] - \frac{24200}{3} - \frac{520}{3}\pi^2\xi - 32\pi^2\xi^2 + \frac{848}{3}\pi^2 - 60\xi + \frac{3584}{3}\xi^2$
(w)	$-\frac{1}{2}C_FC_A$	$\frac{1}{\epsilon^2} [48 + 72\xi + 24\xi^2] + \frac{1}{\epsilon} [408 + 540\xi + 168\xi^2] + \frac{7420}{3} - 96\zeta_3\xi - 192\zeta_3 - 144\pi^2\xi - 48\pi^2\xi^2 - 96\pi^2 + 3058\xi + \frac{2732}{3}\xi^2$
(x)	$-\frac{1}{2}C_FC_A$	$\frac{1}{\epsilon^2} [-48\xi - 24\xi^2] + \frac{1}{\epsilon} [-96 + 32\pi^2\xi + 64\pi^2 - 432\xi - 176\xi^2] - 960 + 480\zeta_3\xi + 1152\zeta_3 + \frac{784}{3}\pi^2\xi + \frac{160}{3}\pi^2\xi^2 + 432\pi^2 - \frac{704}{45}\pi^4 - \frac{8008}{3}\xi - 968\xi^2$
(y)	$T_RC_F$	$\frac{1}{\epsilon^2} [-32] + \frac{1}{\epsilon} [-352] - \frac{6544}{3} + \frac{32}{3}\pi^2$
(z)	$T_RC_F$	$\frac{1}{\epsilon} [16] + \frac{392}{3}$
(aa)	$T_RC_F$	$\frac{1}{\epsilon^2} [\frac{64}{3}] + \frac{1}{\epsilon} [\frac{1024}{9} + \frac{256}{9}\pi^2] + \frac{12928}{27} + \frac{1792}{3}\zeta_3 + \frac{3968}{27}\pi^2$
(ab)	$T_RC_F$	$\frac{1}{\epsilon^2} [-64] + \frac{1}{\epsilon} [-\frac{1024}{3}] - \frac{21608}{15} + 64\pi^2$
(ac)	$T_RC_F$	$\frac{1}{\epsilon} [16] + \frac{32}{15}$
(ad)	$T_RC_F$	$\frac{1}{\epsilon^2} [\frac{64}{3}] + \frac{1}{\epsilon} [\frac{1024}{9} + \frac{256}{9}\pi^2] + \frac{348752}{405} + 256\zeta_3 - \frac{64}{27}\pi^2$

TABLE I: Imaginary parts of three-loop self-energy diagrams in a general covariant gauge (cont).